



**HAL**  
open science

## Prototype Combined Heater/Thermoelectric Power Generator for Remote Applications

Daniel Champier, C. Favarel, Jean-Pierre Bedecarrats, Tarik Kousksou, J. F Rozis

► **To cite this version:**

Daniel Champier, C. Favarel, Jean-Pierre Bedecarrats, Tarik Kousksou, J. F Rozis. Prototype Combined Heater/Thermoelectric Power Generator for Remote Applications. *Journal of Electronic Materials*, 2013, 42 (7), pp.1888-1899. 10.1007/s11664-012-2459-x . hal-02014177

**HAL Id: hal-02014177**

**<https://hal.science/hal-02014177>**

Submitted on 7 Nov 2019

**HAL** is a multi-disciplinary open access archive for the deposit and dissemination of scientific research documents, whether they are published or not. The documents may come from teaching and research institutions in France or abroad, or from public or private research centers.

L'archive ouverte pluridisciplinaire **HAL**, est destinée au dépôt et à la diffusion de documents scientifiques de niveau recherche, publiés ou non, émanant des établissements d'enseignement et de recherche français ou étrangers, des laboratoires publics ou privés.

# Prototype Combined Heater/Thermoelectric Power Generator for Remote Applications

D. CHAMPIER,<sup>1,4</sup> C. FAVAREL,<sup>1,2</sup> J. P. BÉDÉCARRATS,<sup>2</sup> T. KOUSKSOU,<sup>1</sup>  
and J. F. ROZIS<sup>3</sup>

1.—Laboratoire des Sciences de l'Ingénieur Appliquées à la Mécanique et au Génie Electrique (SIAME), Univ Pau & Pays Adour, Hélio parc 2, Avenue du Président Angot, 64053 Pau Cedex, France. 2.—LaTEP—EA 1932, Laboratoire de Thermique, Energétique et Procédés, ENSGTI, Univ Pau & Pays Adour, Rue Jules Ferry, BP 7511, 64075 Pau, France. 3.—Planète Bois, 17 Route de Toulouse, 65690 Barbazan Debat, France. 4.—e-mail: daniel.champier@univ-pau.fr

This study presents a prototype thermoelectric generator (TEG) developed for remote applications in villages that are not connected to the electrical power grid. For ecological and economic reasons, there is growing interest in harvesting waste heat from biomass stoves to produce some electricity. Because regular maintenance is not required, TEGs are an attractive choice for small-scale power generation in inaccessible areas. The prototype developed in our laboratory is especially designed to be implemented in stoves that are also used for domestic hot water heating. The aim of this system is to provide a few watts to householders, so they have the ability to charge cellular phones and radios, and to get some light at night. A complete prototype TEG using commercial (bismuth telluride) thermoelectric modules has been built, including system integration with an electric DC/DC converter. The DC/DC converter has a maximum power point tracker (MPPT) driven by an MC9S08 microcontroller, which optimizes the electrical energy stored in a valve-regulated lead-acid battery. Physical models were used to study the behavior of the thermoelectric system and to optimize the performance of the MPPT. Experiments using a hot gas generator to simulate the exhaust of the combustion chamber of a stove are used to evaluate the system. Additionally, potential uses of such generators are presented.

**Key words:** Thermoelectric generator, maximum power point, MPPT, power generation, biomass stove

## INTRODUCTION

According to the International Energy Agency,<sup>1,2</sup> 1.4 billion people live without electricity, most of them in developing countries. They rely on biomass such as wood, charcoal, agricultural waste, and animal dung to meet their energy needs for cooking. Biomass is burned in an open fire, making an important contribution to household air pollution. According to the World Health Organization, use of wood fuel and dung for cooking and heating causes over 400,000 premature deaths in India annually,

mostly women and children; For example, the concentration of airborne particulate matter in Indian household air using biomass is over 2000  $\mu\text{g}$  per cubic meter, compared with the US limit of 150.<sup>3-6</sup>

To avoid this air pollution, the first thing to do is to use a stove instead of an open fire. To be efficient, stoves need tall flues to generate adequate draw. These flues are expensive and time-consuming to build. In some countries, with flat roofs, people do not have the technology to build chimneys going through the roof.

The possibility of adding an electric fan dramatically increases the widespread use of stoves. Addition of a fan greatly improves the overall performance of cooking stoves: it improves the air-to-fuel ratio,

(Received July 7, 2012; accepted December 28, 2012)



Journal : 11664\_JEM

Article No.: 2459

Dispatch : 22-1-2013

LE  
 CP

Pages : 12

TYPESET  
 DISK

61 allowing far better combustion, and the total heat  
62 recovery can be improved because the combustion  
63 gases do not need to be at a high temperature.

64 Improving the efficiency and quality of combus-  
65 tion contributes to reducing outside air pollution  
66 and to reducing the quantity of wood used, which is  
67 especially important in areas where wood is scarce.

68 When a household gains access to electricity, the  
69 normal first use is as a kerosene or biomass sub-  
70 stitute for lighting, extending working hours in the  
71 evening or night. The other basic needs are mainly  
72 radio and cellular phone charging (overall telephone  
73 ownership in India reached 74% at the end of June  
74 2011<sup>7</sup>).

75 Connecting these households previously without  
76 electricity to the power grid would mean two  
77 important costs for remote villages: the cost of  
78 building new landlines and the cost of electricity  
79 distribution.

80 A study conducted by the International Bank for  
81 Reconstruction and Development<sup>8</sup> shows that the  
82 cost of connecting houses to the grid in Bahia  
83 (Brazil) depends considerably on the distance of the  
84 village from the grid and on the number of utility  
85 poles per consumer, and also on the terrain (flat or  
86 hilly). The average cost of connecting households is  
87 more than US \$300, assuming one utility pole per  
88 consumer. The more scattered the households are  
89 (villages with more than two utility poles per con-  
90 sumer), the more the costs increase (more than  
91 US \$1000 for a distance of less than 1 km to the  
92 grid). For four poles per consumer the cost explodes  
93 to more than US \$4000, justifying the search for  
94 alternative methods of generating electricity.

95 The cost of transmission and distribution of elec-  
96 tricity in India has been studied by Nouni et al.<sup>9</sup> It  
97 varies from US \$0.07 to US \$5.1 per kWh depend-  
98 ing on the peak electrical load and the load factor.  
99 The worst case was for a distance of 20 km between  
100 the village and an existing 11-kV line, a peak load of  
101 5 kW, and a load factor of 0.1 (where electricity  
102 would be mainly required for lighting in the evening  
103 for a few hours). These villages built on hilly ground  
104 have a relatively lower number of households.  
105 Moreover, most of them have no industrial or com-  
106 mercial load.

107 This result clearly indicates that providing elec-  
108 tricity through grid connectivity to small remote  
109 villages in hilly and other inaccessible areas where  
110 people have very low income is financially unviable.  
111 Renewable energy technologies such as solar, wind,  
112 and thermoelectric generators (TEGs) are cost-  
113 effective options for these specific off-grid house-  
114 holds.

115 Small TEG prototypes with optimized DC/  
116 DC convertors (Fig. 1) have been studied in our  
117 laboratory. These TEGs are one of the solutions for  
118 these households far from the power grid. Coupled  
119 with clean and efficient cooking stoves developed by  
120 Planète Bois (Fig. 2), TEGs can provide electricity  
121 in order to improve the combustion and to respond

122 to basic household needs [light-emitting diodes  
123 (LEDs), cell phone and radio charging devices].  
124 Planète Bois, a nongovernmental organization, aims  
125 to transfer recent knowhow in biomass combustion  
126 and in use of traditional materials (lime, hay, sand,  
127 and straw) to promote the use of low-cost and highly  
128 efficient stoves for household and small-scale  
129 industries, mainly in rural areas.

130 Figure 2 shows a schematic drawing of the  
131 energy-efficient, multifunction, mud stove devel-  
132 oped by Planète Bois. The wood in the pyrolysis  
133 chamber rests on a bed of embers fed by the entry of  
134 primary air at this level. Combustible gases are  
135 given off as a result of decomposition by heat (pyro-  
136 lysis) in the absence of flames and sucked towards a  
137 nozzle. Then, these gases are mixed with the oxygen  
138 from the secondary air. The flame then breaks out  
139 downstream of the injection of secondary air. The  
140 smoke extractor fan allows control of the air-to-fuel  
141 ratio and therefore optimizes the combustion. The  
142 fan also permits the use of a horizontal pipe,  
143 avoiding the necessity for long metal flue pipes and  
144 building of chimneys. The idea is to put the TEG in  
145 a cogeneration system which simultaneously pro-  
146 vides electric power and useful heat for hot water.<sup>10</sup>  
147 Measurements made with a 10-kW wood-burning  
148 cooking stove developed by Planète Bois showed  
149 that about 2.4 kW is used to heat up domestic hot  
150 water. This heat flux from the hot gases to the water  
151 will provide the temperature difference through the  
152 TE modules.

153 A prototype TEG (consisting of one or two com-  
154 mercial bismuth telluride modules) has been  
155 designed and tested with a gas heater providing a  
156 flux similar to the one of the cooking stove. The  
157 mechanical and thermal parts of this prototype have  
158 already been described.<sup>11</sup>

159 During combustion, the temperature of the com-  
160 bustion gases varies significantly (fire ignition,  
161 wood loading, presence or absence of pans on the  
162 hotplate, and quality of wood). Furthermore, the  
163 water temperature increases slowly but can vary  
164 quickly when the user takes hot water and adds cold  
165 water to the tank. For these reasons, the tempera-  
166 ture difference fluctuates a lot during use of the  
167 stove.

168 Thermoelectric modules are made of  $n$  couples of  
169  $p$ -type and  $n$ -type semiconductor pellets connected  
170 with metal solder. They can be represented by a  
171 voltage source with an internal resistance. The  
172 voltage source is approximately proportional to  
173 the temperature difference between the two sides of  
174 the thermoelectric elements:  $E_{oc} = n\alpha_{pn}(T_{hot} - T_{cold})$ ,  
175 and the internal resistance  $R_i = n[(\rho_n \times L_n/S_n)$   
176  $+ (\rho_p \times L_p/S_p)] + R_c$  is also correlated with temper-  
177 ature.  $T_{cold}$  and  $T_{hot}$  are, respectively, the cold- and  
178 hot-side temperatures of the TE modules, and  $n$  is  
179 the number of semiconductor couples.

180  $L_n$ ,  $L_p$  and  $S_n$ ,  $S_p$  are, respectively, the leg length  
181 and cross-sectional area of the pellets.  $\rho_p$  and  $\rho_n$   
182 are the resistivity of each material, and  $\alpha_{pn}$  is the



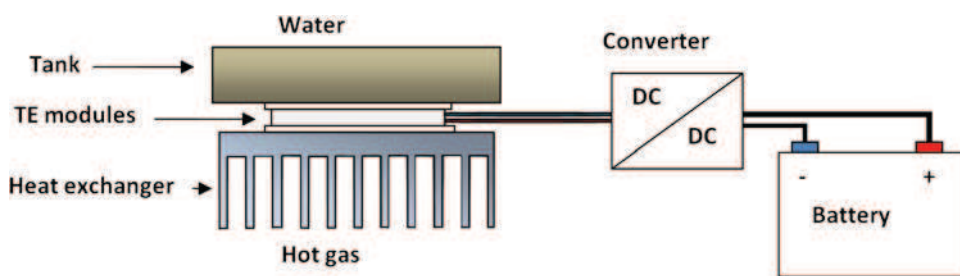


Fig. 1. Prototype TEG with optimized DC/DC converter, for use with hot gas source and cold water sink.

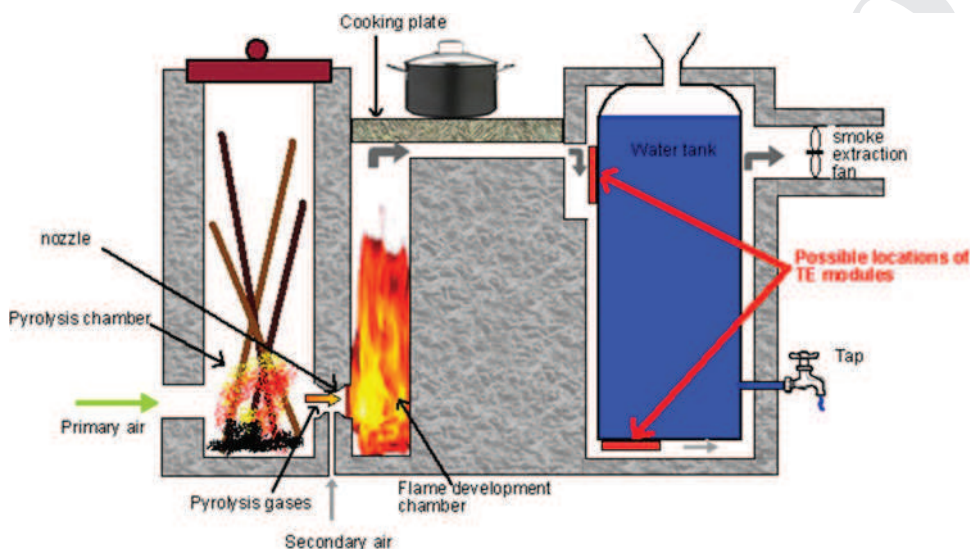


Fig. 2. Planète Bois cooking/water heating stove design.

183 Seebeck coefficient of the couple; these parameters  
 184 are temperature dependent.  $R_c$  represents all the  
 185 electrical contact resistances.

186 Figure 3 shows the variations of the output volt-  
 187 age and of the temperatures for a 1-h experiment  
 188 based on typical use of the cooking stove.

189 Because of this huge variation, a DC/DC con-  
 190 verter (Fig. 4) is necessary to regulate the voltage  
 191 and to store electricity in a battery in order to have  
 192 electricity available all day long, as the TEG only  
 193 produces when the stove is working. To get the  
 194 maximum power from the TE modules, the load  
 195 should be adapted, which means that the impedance  
 196 seen by the TEG is equal to its internal resistance.  
 197 As the current in the battery depends on the battery  
 198 charging but also on the variation of the load, the  
 199 output current and thus the input current of the  
 200 DC/DC converter will fluctuate a lot. With a fixed  
 201 output voltage the load would not be adapted and  
 202 the efficiency would be low. To be always adapted,  
 203 the solution is to control a DC/DC converter with a  
 204 maximum power point tracker (MPPT). This can be  
 205 done by adding a microcontroller which controls the  
 206 output power of the converter.

207 The next section describes the DC/DC controller  
 208 and the use of the MPPT algorithm. Special attention

209 has been paid to the choice of electronic components  
 210 in order to increase the internal efficiency of the DC/  
 211 DC controller. The MPPT algorithm efficiency has  
 212 also been studied using a Matlab–Simulink model  
 213 including measurement noise in order to determine  
 214 the best tracking increment value (or rather range).  
 215 The overall electrical efficiency between the output  
 216 power of the TE module and the power at the battery  
 217 terminals is presented. The test of the DC/DC con-  
 218 troller is presented in the following section. In the last  
 219 section, the first experimental results obtained with a  
 220 hot gas generator simulating the exhaust of the  
 221 combustion chamber of a cooking stove are shown.  
 222 The final stored electrical power results are pre-  
 223 sented, and the energy efficiency between the elec-  
 224 trical energy given by the TE modules and the energy  
 225 storage in the battery is measured. Based on these  
 226 results, the daily electrical production of the multi-  
 227 function cooking stove and its possible uses are  
 228 evaluated.

### DC/DC CONVERTER

229  
 230 The study that was done to maximize the perfor-  
 231 mance of the DC/DC converter is presented in this

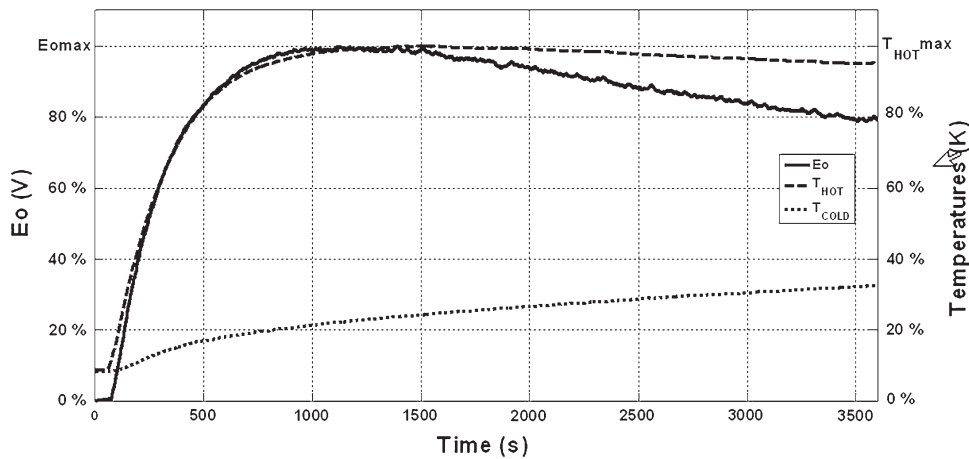


Fig. 3. Typical variations of the output voltage and temperatures of the TEG.

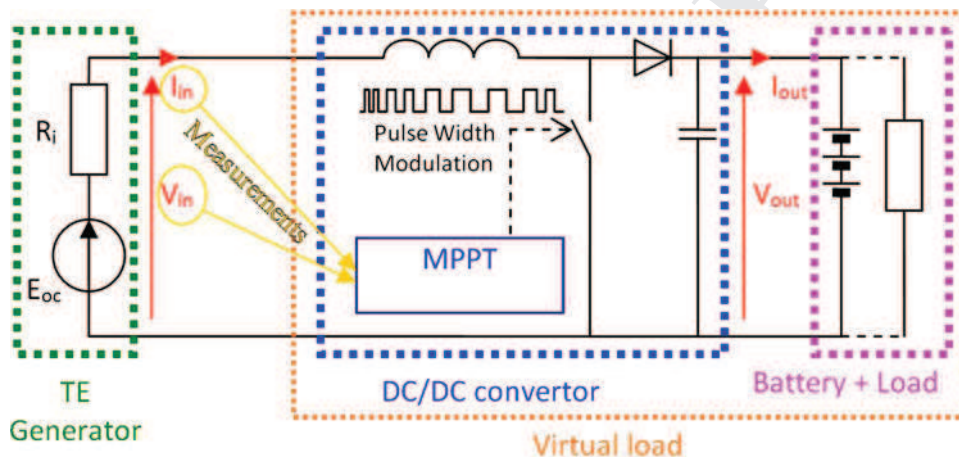


Fig. 4. Global electric circuit of the TEG with its storage battery and load.

section. The power efficiency can be defined as the ratio of the power stored in the battery to the maximum power that the thermoelectric module can provide for a specific operating point. The energy efficiency can be defined as the ratio of the energy stored in the battery to the maximum energy that the thermoelectric module can provide during typical use of the stove. The goal is to optimize energy efficiency.

The design of the converter can be separated into two stages: first the electrical components part which gives us the DC/DC efficiency, then the algorithmic part which represents the MPPT efficiency. This study is divided into two stages, because the total efficiency is the result of the following product: Efficiency = MPPT efficiency × electronic efficiency, which can be studied separately.

For this application, a boost converter has been used (Fig. 4).  $V_{in}$  and  $I_{in}$  are, respectively, the input voltage and current of the DC/DC converter.  $V_{out}$

and  $I_{out}$  are, respectively, the output voltage and current of the DC/DC converter.

### Principle of the MPPT

#### Description of the MPPT Algorithm

The TE module with the DC/DC converter and the load is illustrated by Fig. 5. The electrical power ( $P_{in}$ ) characteristic of the TE modules as a function of the voltage is plotted in Fig. 6 for several values of the temperature difference between the two sides of the TE modules. These curves, typical of TE modules, show that the voltage  $V_{in}$  must be adapted in order to get the maximum power. The maximum power point (MPP) changes with the temperature difference, which is why a management algorithm is necessary.

The parameter driven by the microcontroller is the duty cycle (Dc) of the pulse width modulation, which is the fraction of the commutation period  $T$  during which the switch is on. Assuming an ideal

270 converter (without losses) the relations governing  
 271 the system are:

$$I_{in} = \frac{I_{out}}{(1 - Dc)} \dots V_{in} = V_{out} \times (1 - Dc) \dots P_{in}$$

$$= V_{in} \times I_{in} = V_{out} \times I_{out} = P_{out}.$$

273  $P_{out}$  is the electrical power output of the DC/DC  
 274 converter.

275 It is reasonable to consider that  $V_{out}$  is fixed by  
 276 the battery voltage, therefore the choice of Dc im-  
 277 poses the voltage  $V_{in}$  and as a consequence the  
 278 currents.

279 A simple MPPT algorithm strategy making  $V_{in}$   
 280 equal to  $E_{oc}/2$  could not be used in this study be-  
 281 cause  $E_{oc}$  fluctuates a lot with temperature. Another  
 282 strategy based on tracking the internal resistance is  
 283 not possible since this internal resistance is also a  
 284 function of the temperature.

285 The solution is to measure both  $V_{in}$  and  $I_{in}$  in  
 286 order to determine the electrical power and to

adjust Dc in order to maximize this value. The  
 perturb and observe (P&O) method which maxi-  
 mizes the input power ( $P_{in}$ , the power generated by  
 the TEG) without any knowledge of the source is  
 chosen for the MPPT. The principle (Fig. 7) is to  
 alter the voltage  $V_{in}$  by a small amplitude (obtained  
 by changing Dc slightly) around its initial value and  
 analyze the behavior of the  $P_{in}$  power variation that  
 results. If a positive increment of the voltage  $V_{in}$   
 causes an increased power  $P_{in}$ , this means that the  
 operating point is on the left of the MPP. If the  
 power decreases, this implies that the system has  
 exceeded the MPP. A similar analysis can be done  
 when the voltage decreases. From these various  
 analyses of the consequences of changing voltage on  
 the characteristic  $P_{in} = f(V_{in})$ , it is easy to locate the  
 operating point from the MPP. Then, appropriate  
 control will allow convergence to the maximum power.

The algorithm is described in Fig. 7. The fre-  
 quency of the algorithm was fixed at 1 Hz for all the  
 analyses.

$V_{in}$  and  $I_{in}$  are measured using the analog-  
 to-digital converter inputs of the microcontroller.  
 Measurement of  $V_{out}$  is also necessary to incorpo-  
 rate battery protection in order to increase its life  
 expectancy. Moreover, to avoid problems due to  
 noise at low measurement values, we decided that,  
 for input power less than 1 W, the algorithm does  
 not start and the Dc is fixed.

*Efficiency Analysis and Optimization*

The principal limitation of the P&O method<sup>13</sup> is  
 the oscillations around the maximum power which  
 decrease the MPPT efficiency. The amplitude of  
 these oscillations, which depends on the noise  
 measurements ( $\Delta I_{in}$  and  $\Delta V_{in}$ ) and on the input  
 voltage values, can be minimized by choosing an  
 optimized Dc increment  $\Delta Dc$ .

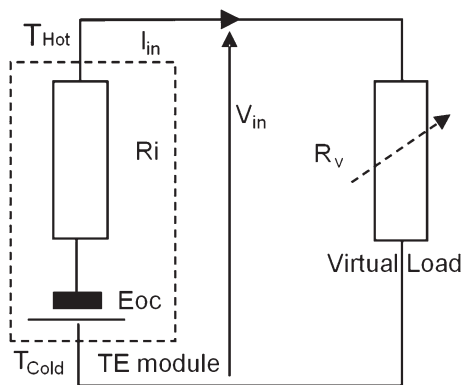


Fig. 5. Electrical model of the TE module and the DC/DC virtual load.

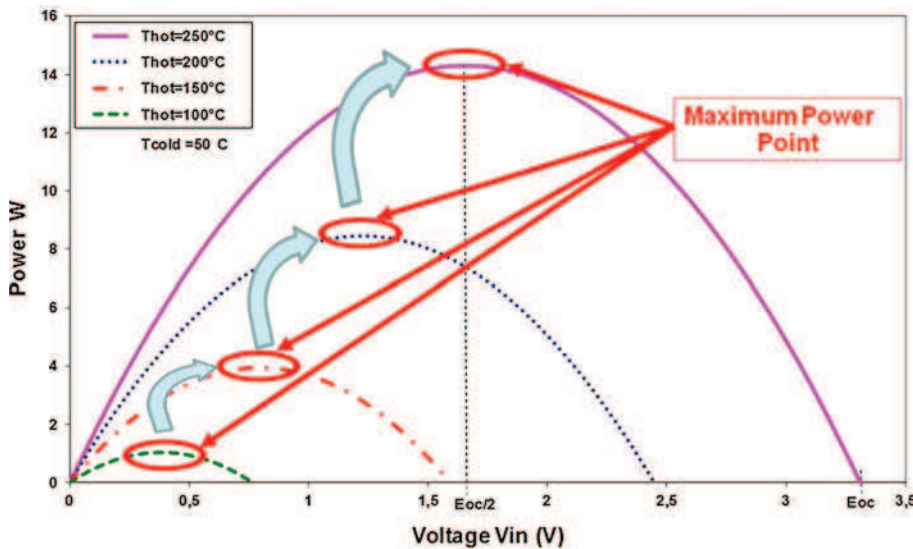


Fig. 6. TE module output power as a function of the TE voltage for different temperatures.

Author Proof

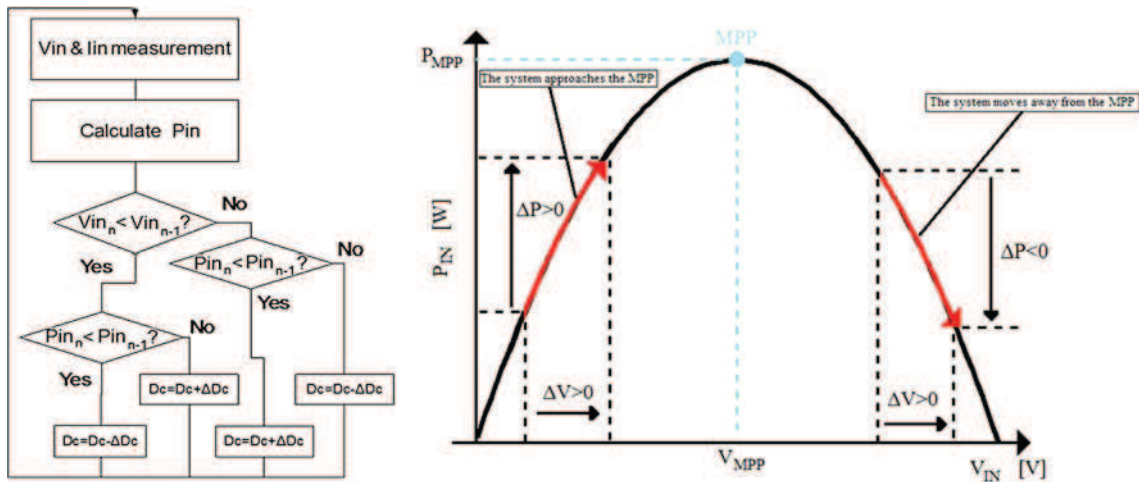


Fig. 7. Principle of MPPT with its algorithm.

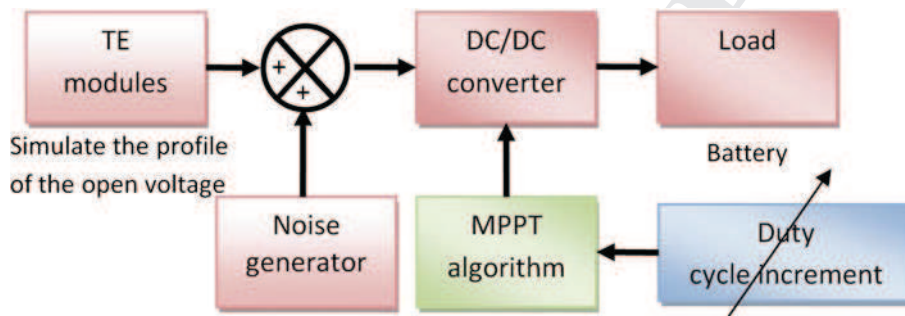


Fig. 8. Simulink model of the TE generator with its load.

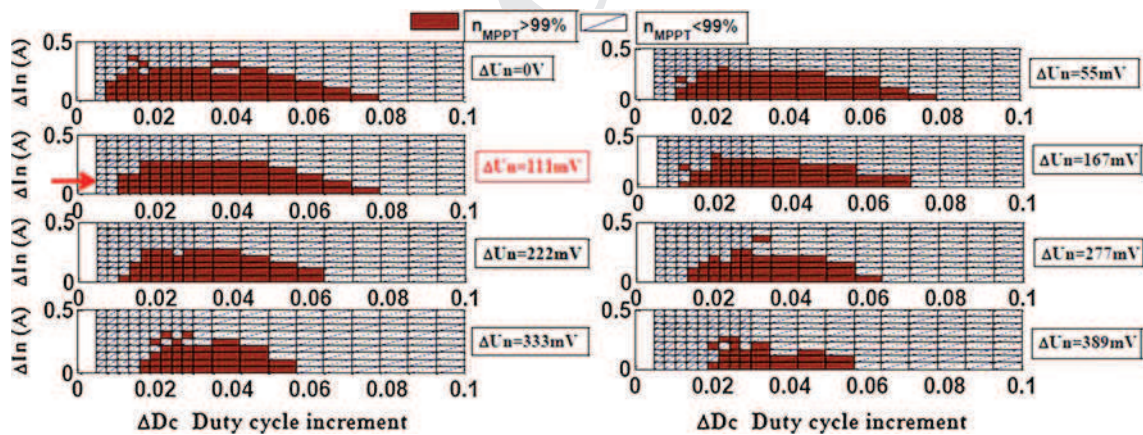


Fig. 9. Influence of noise ( $\Delta I_n$  and  $\Delta V_n$ ) on the energy efficiency of the P&O algorithm.

Two analyses were carried out using a Simulink model (Fig. 8), the first one taking into account the impact of the noise on the current and voltage measurements, and a second analysis taking into account the influence of the maximum open-circuit voltage.

To carry out a realistic analysis, the cycle of Fig. 3 based on typical use of the cooking stove was used for the TE modules block. A noise generator added

random noise (white noise) on  $V_{in}$  and  $I_{in}$ . A heat cycle of 1 h is considered. The typical value of the open-circuit voltage reached during the typical cycle  $E_{omax}$  is 9.2 V (corresponding to 10 W), but it was used as a parameter in our study.

The first analysis presents the influence of the Dc increment choice for different noise values on the efficiency. Noise can originate in the environment of the system, but it mainly comes from the DC/DC

333  
334  
335  
336  
337  
338  
339  
340  
341

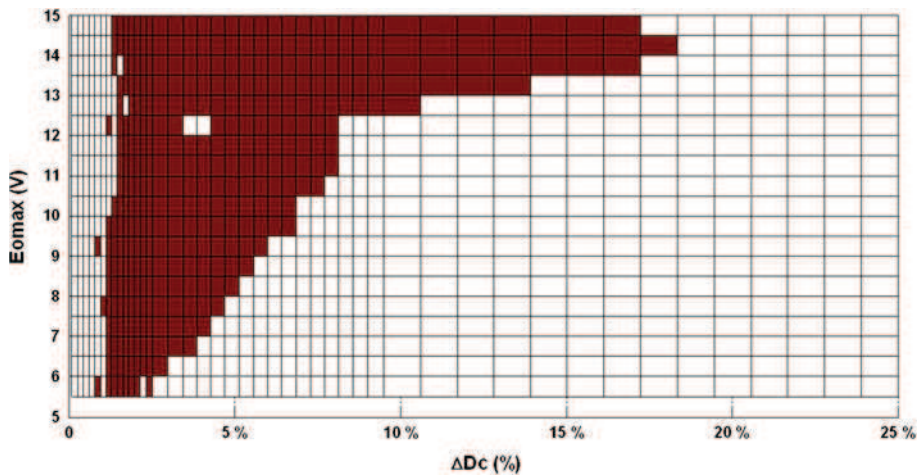


Fig. 10. Influence of the maximum open-circuit voltage on the energy efficiency of the P&O algorithm for different increments of Dc.

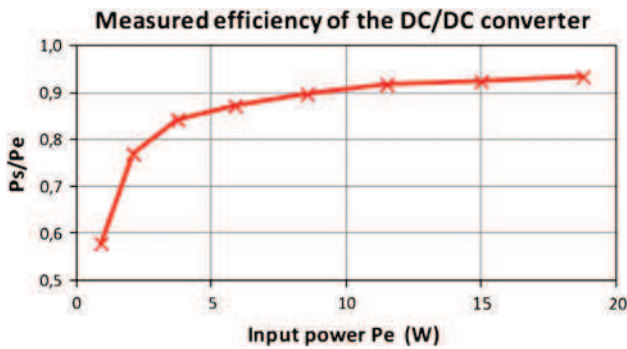


Fig. 11. Electronic power efficiency of the DC/DC converter.

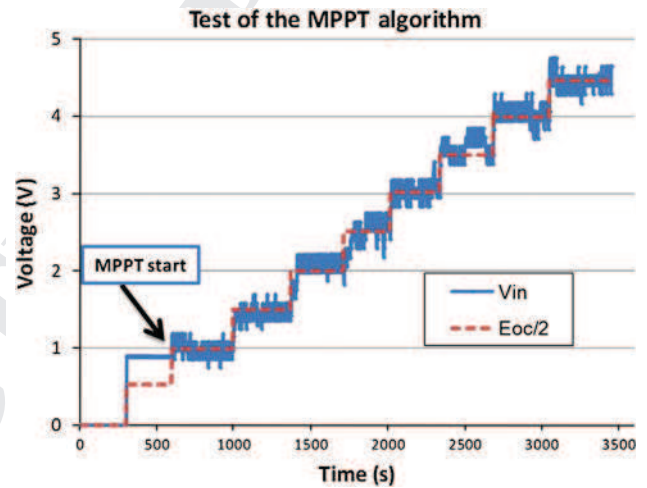


Fig. 12. Test of the P&O algorithm.

342 converter. The DC/DC converter works at about  
 343 100 kHz, and the maximum commuted voltage and  
 344 current are, respectively, 7 V and 3 A, so the noise  
 345 cannot be avoided. The Simulink model was run ten  
 346 times for each point, and the energy efficiency over  
 347 the entire cycle was calculated.

348  $\Delta Dc$  is a crucial parameter in choosing a trade-off  
 349 between speed and oscillations. If  $\Delta Dc$  is too small,  
 350 in case of quick variations of the variables (mainly  
 351 input voltage and output current), the algorithm is  
 352 slow to reach the MPP. If  $\Delta Dc$  is too big, the algo-  
 353 rithm oscillates too much around the MPP at  
 354 steady-state operation.

355 The results presented in Fig. 9 (MPPT efficiency  
 356 over 99% is in brown and below 99% in white) show  
 357 that the brown area decreases when the noise vol-  
 358 tage increases. In the case of unknown noise sources,  
 359 the Dc increment has to be chosen between 2% and  
 360 5% in order to maximize efficiency.

361 The second analysis was performed to evaluate  
 362 the effects of variation of the maximum open-circuit  
 363 voltage.

364 In winter, according to Planète Bois, the hot  
 365 water needs are more important (2.5 kW instead of  
 366 1.75 kW), so the heat flux increases, and the voltage  
 367 of the TE modules increases. Moreover, the ageing

of various materials and the installation of the  
 system may also change the operating point. To  
 study this influence, we chose to keep the same  
 curve shape (Fig. 3) and to vary the maximum value  
 of the open-circuit voltage  $E_{omax}$ . This is why an  
 analysis on the impact of the maximum open-volt-  
 age was carried out.

In our prototype, the noise is the result of the  
 voltage and current commutations at 100 kHz of  
 the DC/DC convertor. Measurements show that the  
 voltage noise is around 110 mV and that the current  
 noise is around 110 mA (represented by a red arrow  
 in Fig. 9). It will be the same in isolated houses. The  
 criterion is also to keep the energy efficiency over  
 99%.

The result of the simulation is presented in  
 Fig. 10, where the MPPT efficiency over 99% is in  
 brown and below 99% is in white.  $E_{omax}$  was  
 chosen between 5.5 V and 14 V, because when  
 $E_{omax} < 5.5$  V, the electrical power output is not

368  
 369  
 370  
 371  
 372  
 373  
 374  
 375  
 376  
 377  
 378  
 379  
 380  
 381  
 382  
 383  
 384  
 385  
 386  
 387

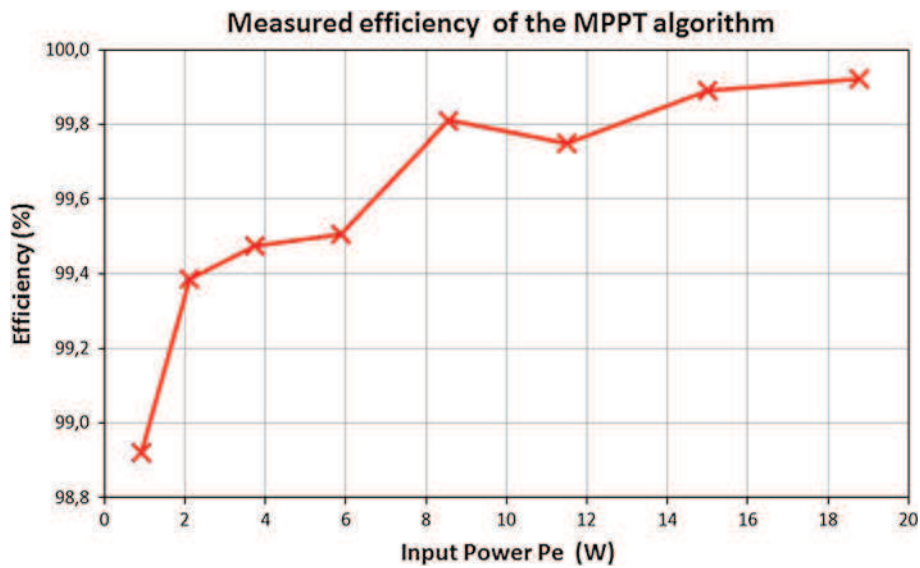


Fig. 13. Measured power efficiency of the P&O algorithm.

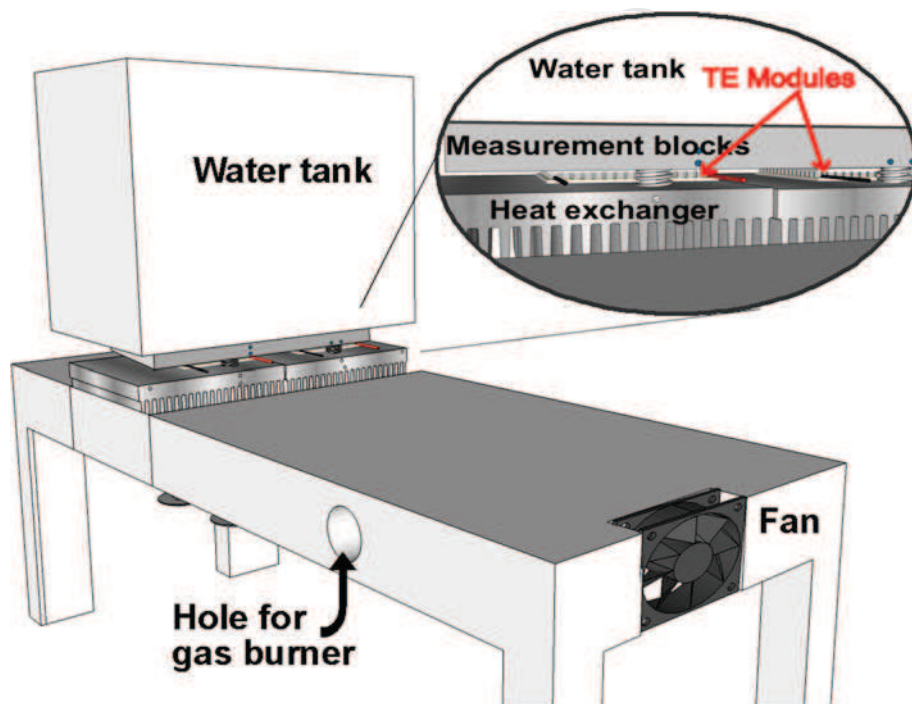


Fig. 14. Test bench for simulating the stove.

388 significant and because 14 V is the maximum value  
 389 for the boost converter.

390 The figure shows that, when the open-circuit  
 391 voltage increases, the area of efficiency up to 99%  
 392 increases. This is due to the oscillation phenome-  
 393 non: at low open-circuit voltage, if the  $D_c$  incre-  
 394 ment is too high, oscillations cause significant losses,  
 395 whereas at high open-circuit voltage, even if  
 396 increasing the  $D_c$  increment increases the oscilla-  
 397 tion losses, 99% is maintained.

Figure 10 clearly demonstrates that the optimal 398  
 value for the increment of  $D_c$  is around 2%, and the 399  
 large area of the graph with acceptable values 400  
 shows that this value is not critical. 401

#### MPPT Conclusion 402

A MPP boost converter dedicated to the TEG has 403  
 been developed. The model-based design of the DC/ 404  
 DC converter, including modeling of noise and using 405

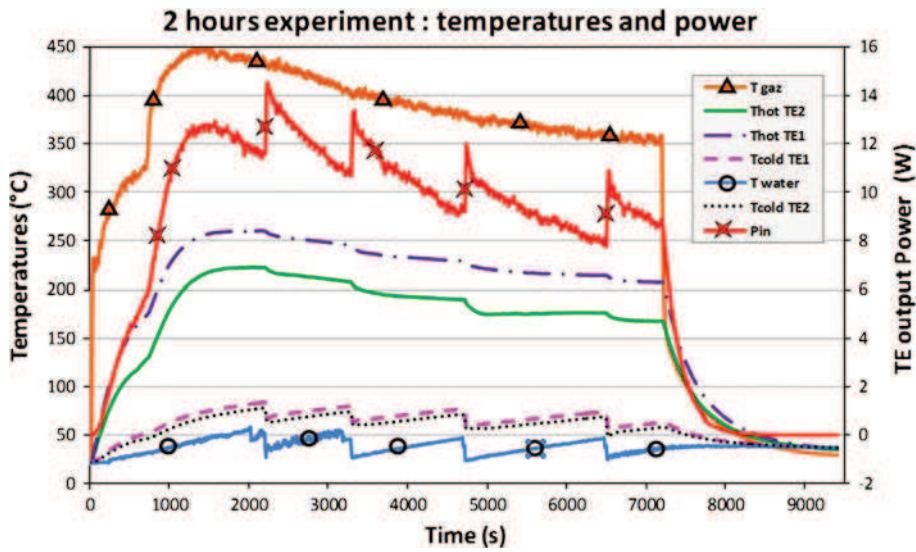


Fig. 15. Temperatures and electrical power of a 2-h experiment of the TEG.

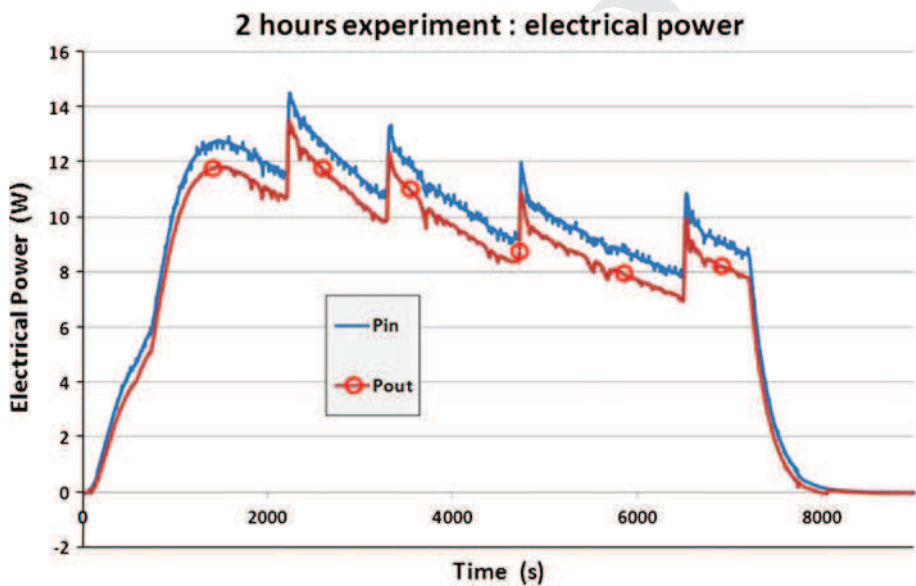


Fig. 16. Input and output electrical power of the DC/DC converter for a 2-h experiment of the TEG.

406 typical measurements of the output voltage of the  
 407 TE generator as inputs, allows the choice of an  
 408 optimal value for the increment of Dc. The design  
 409 shows that, in the case of unknown noise sources,  
 410 the Dc increment has to be chosen between 2% and  
 411 5% to maximize the energy efficiency. When the  
 412 TEG is used in the Planète Bois cooking stove in an  
 413 isolated house, noise will come from the commuta-  
 414 tion of the converter and will be known. In this case,  
 415 a choice of 2% will optimize the converter for all the  
 416 various operating conditions of the stove. With this  
 417 choice of 2% for the Dc increment and with the  
 418 actual thermal cycle, calculations show that we can  
 419 expect a MPPT efficiency of 99.5%.

### Test of the DC/DC Converter

A DC/DC converter driven by an MC9S08 microcontroller was built and tested. The electronic components were chosen in order to have good conversion efficiency. The electronic efficiency of the DC/DC boost converter was tested for different power input values (Fig. 11).

The power efficiency within the normal operating range is better than 90%. This efficiency is limited by the technology of the components and therefore mainly by price.

The MPPT algorithm was installed in the microcontroller. To avoid problems at very low voltages

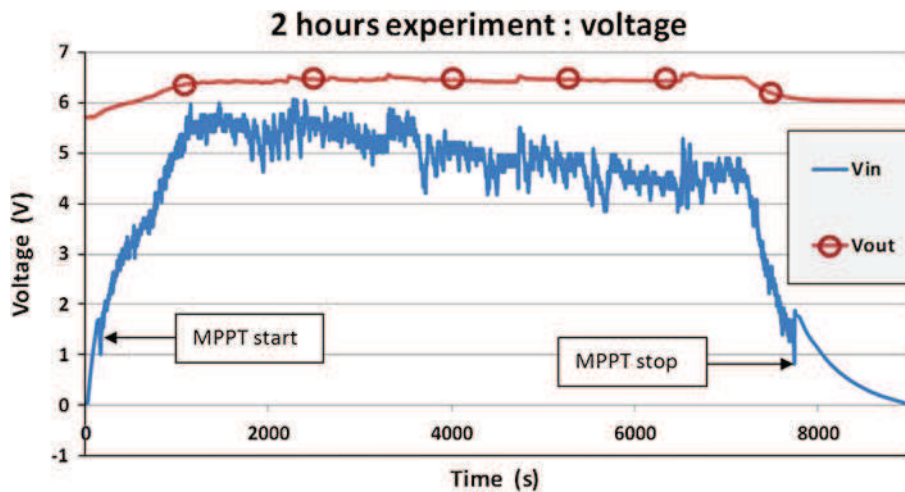


Fig. 17. Input and output voltage of the DC/DC converter for a 2-h experiment of the TEG.

**Table I. Electrical energy produced and its possible uses for different cooking cycles**

| Cycle                         | One Cooking (2 h)                       | Two Cookings per Day                           | Two Cookings (One Long) per Day                 |
|-------------------------------|---|--|---|
| Electrical energy stored (Wh) | 18.2                                    | 36.5   | 54.7  |
| Use example*                  | Fan, one phone charge, and 3 h of light | Fan, two phone charges, and about 6 h of light | Fan, two phone charges, and about 10 h of light |

\* Phone battery of 3.7 V, 1050 mAh. Light consumption of 4 W. Fan 1 W during cooking.

**Table II. Economic study of the TEG**

|                   | <5  | <100 | <1000 |
|-------------------|-----|------|-------|
| Number of systems | <5  | <100 | <1000 |
| Price (€)         | 200 | 120  | 70    |

and currents (mostly because of false measurements due to noise), conditions on the voltage and power level were added to the algorithm. A sleep mode was also added so that there would be no consumption of electrical energy when the TEG is not in use.

The MPPT algorithm was tested using a voltage source  $E_{oc}$  with very low internal resistance. For this reason, a fictitious internal resistance with a value equivalent to the TE module resistance had to be added. Figure 12 shows the evolution of the input voltage of the converter when the open-circuit voltage of the generator was increased in steps. It shows the fluctuations due to the P&O algorithm around the adapted voltage ( $E_{oc}/2$ ).

The power efficiency of the MPPT algorithm was calculated by comparing the measured output power of the converter with the power obtained in the case where the load is perfectly adapted ( $E_{oc}^2/4R_i$ ). The results presented in Fig. 13 show that the goal of energy efficiency above 99% is reached as soon as the input power is significant.

The power consumption in sleep mode was also measured and found to be less than 30 mW.

The next step was to test the energy efficiency of the converter using a typical cycle of the stove.

**TRIAL OF THE COMPLETE TE GENERATOR**

The next step was to test the TE generator with the MPPT DC/DC converter on the prototype TEGBioS (Fig. 1) already described. The two thermoelectric modules ( $Bi_2Te_3$  modules from Thermoamic, reference TEP1-12656-0.6) were connected in series, and pressure of 5 bar was applied to ensure good thermal and electric contacts. Electricity was stored in a 6-V battery. Laboratory testing of the generator was performed using a gas burner, as the installation of a wood stove is not possible in the laboratory premises. A small gas (butane) tank supplies the burner.

The smoke duct which heats the hot water in the cooking stove was replaced by a thermally insulated metal pipe. Heat was generated by a 3-kW gas burner, and the hot gases were blown into the pipe right under the TEG by a fan.

Figure 14 shows a schematic diagram of the test bench used to test the whole system. The fan was set to achieve a gas speed in the duct similar to that of the combustion gases from a cooking stove. The heat source was a moving airstream at about 400°C, and the cold source was a water tank of 9 L. Glass wool (not shown in the schematic diagram) was used as thermal insulation.

483 Temperature, voltage, and current were recorded  
 484 by using an Agilent 34970A data logger. The mea-  
 485 surement system gave precision of  $\pm 0.01\%$  for the  
 486 voltage,  $\pm 0.1\%$  for the current, and  $\pm 0.5^\circ\text{C}$  for the  
 487 temperature.

488 A typical 2-h cooking experiment was carried out.  
 489 The test protocol respected the traditional use of the  
 490 cooking stove. The hot water tank was emptied as  
 491 soon as its temperature reached  $50^\circ\text{C}$ , being refilled  
 492 with cold water. This was done four times during  
 493 the cooking. The results are presented in Fig. 15.

494 The temperatures  $T_{\text{hotTE1}}$ ,  $T_{\text{hotTE2}}$ ,  $T_{\text{coldTE1}}$ ,  
 495 and  $T_{\text{coldTE2}}$  were measured on the heat  
 496 exchangers near the hot and cold sides of the two TE  
 497 modules. The difference between the two modules is  
 498 due to the slight asymmetry of the burner. The  
 499 temperature of the gas was measured just before the  
 500 heat exchanger in the middle of the hot gas flow.  
 501 The plotted temperature of the water was measured  
 502 at the bottom of the tank (it was measured to be 5 K  
 503 to 7 K less at the top, but this is not plotted).

504 The temperature of the gas decreased slowly be-  
 505 cause of the decrease in the butane flow in the  
 506 burner (reduction in pressure in the cylinder of  
 507 butane gas during the experiment), but the experi-  
 508 ment is still representative of a cooking period.

509 The power generated by the two TE modules ( $P_{\text{in}}$ )  
 510 and also the power output ( $P_{\text{out}}$ ) of the DC/DC con-  
 511 vector are plotted in Fig. 16. Peak power occurs  
 512 immediately after changing the water in the tank.  
 513 Fluctuations in power due to the algorithm and  
 514 noise are visible in the figure as expected from the  
 515 simulation. The maximum power reaches about  
 516 14.5 W on the input side of the converter.

517 Figure 17 shows the startup of the MPPT algo-  
 518 rithm. The converter works at a constant Dc until  
 519 1 W is reached. At this time, the input voltage  
 520 decreases quickly to  $E_{\text{oc}}/2$  and then follows this  
 521 value, which increases with the temperature dif-  
 522 ference. After the end of the combustion cycle, the  
 523 MPPT stops at the same value and then the DC/DC  
 524 controller goes into sleep mode.

525 The measurements shown in Fig. 16 allow calcula-  
 526 tion of the energy produced by the TE modules and  
 527 stored in the battery by integrating the curve. Then,  
 528 the electronic energy efficiency of the DC/DC convertor  
 529 can be calculated and was found to be equal to 90.7%.

530 Multiplying this efficiency by the efficiency of  
 531 Fig. 13 we obtain the global energy efficiency of the  
 532 DC/DC converter, which is around 90%.

533 It is also possible to evaluate the efficiency of the  
 534 thermoelectric modules by measuring the heat  
 535 transmitted to the water during the experiment.  
 536 Assuming that the heat converted to electrical  
 537 power is negligible, and if we neglect the losses  
 538 around the water tank, this heat is the energy  
 539 entering the TE modules. An efficiency of 2% was  
 540 measured. This efficiency is low, but one must keep  
 541 in mind that the energy that flows through the  
 542 generator is not wasted because it is used to heat  
 543 water in the tank.

From this experiment, it is possible to predict the  
 electrical energy produced each day depending on  
 the lifestyle of the inhabitants. Cooking techniques  
 vary widely across the world; for example, simmer-  
 ing lasts far longer than grilling. Two lifestyles were  
 considered: 1 day including two short cooking peri-  
 ods of 2 h, one in the morning and one in the  
 afternoon, and 1 day including one short cooking  
 period in the morning and a 4-h cooking period in  
 the afternoon (representing the preparation of a  
 dish such as a tajine in rural Morocco, for example).  
 The nature of the cooking style has little influence  
 on the operation of the stove. The heat radiated by  
 the cooking plate is very important, and the effect of  
 adding a pan does not really modify the production  
 of hot water and therefore the production of elec-  
 tricity. Time is the main parameter for electricity  
 generation.

The use of the produced electrical energy was  
 then distributed in the following manner over a  
 period of 24 h: circuit power consumption in sleep  
 mode (30 mW) outside the period of cooking, con-  
 sumption of the fan (1 W) during cooking times, one  
 or two charges of a mobile phone, and the rest in  
 light with 4-W LEDs. The results are presented in  
 Table I.

As this TEG is for people with low income, these  
 results were completed with an economic study as  
 presented in Table II; the price includes the cost of  
 the TE modules, the heat exchanger, and the DC/DC  
 converter. The price decreases mostly with the  
 number of units, due to the reduction in price of the  
 TE modules when they are bought in large quantities.

The promising results of Table I combined with  
 the reasonable cost in Table II show that the use of  
 TE modules on cooking stoves should enable people  
 living in isolated houses to have light for several  
 hours in the evening and to charge their phones. Of  
 course it also permits the use of improved cooking  
 stoves with a fan, allowing almost perfect combus-  
 tion. TEGs are a potentially important contributor  
 to the supply of electricity to rural areas.

## CONCLUSIONS

In this paper, optimization of the electric part of a  
 TEG designed for cogeneration in efficient cooking  
 stoves has been presented. The DC/DC converter  
 uses a P&O MPPT algorithm in order to always  
 match the load to the fluctuating characteristics of  
 the TE modules due to the temperature variation. A  
 model-based design of the DC/DC converter was  
 conducted to determine the increment of Dc of the  
 MPPT algorithm that optimizes the energy effi-  
 ciency of the converter. With the optimized incre-  
 ment, the MPPT algorithm shows energy efficiency  
 over 99%, which gives global energy efficiency for  
 the electrical convertor of over 90%. A first experi-  
 ment made with a hot gas generator simulating the  
 exhaust of the combustion chamber inside a cooking  
 stove allowed the evaluation of the potential of this

Author Proof



603 system. This TEG is certainly a low-cost solution for  
 604 houses that are far from the electrical power grid in  
 605 developing countries. This TEG has been developed  
 606 to be combined with a stove designed by Planète  
 607 Bois; however, it can be easily adapted to be used in  
 608 stoves that have a hot water tank. Its use is not  
 609 limited to developing countries but could also be  
 610 adapted to make autonomous high-technology  
 611 stoves requiring some electronic control.

#### 612 ACKNOWLEDGEMENTS

613 The authors acknowledge the financial support of  
 614 the Conseil Régional d'Aquitaine and of the Conseil  
 615 Général des Pyrénées Atlantiques.

#### 16 REFERENCES

- 17 1. World Energy Outlook WEO-2010, Energy poverty—how to  
 18 make modern energy access universal? (Paris: International  
 19 Energy Agency Publications, 2010). [http://www.iea.org/  
 20 publications/freepublications/publication/weo2010\\_poverty.  
 21 pdf](http://www.iea.org/publications/freepublications/publication/weo2010_poverty.pdf).
- 22 2. World Energy Outlook WEO-2007 (Paris: International  
 23 Energy Agency Publications, 2007), Chap 20, ISBN: 978-92-  
 24 64-02730-5.
3. A.N. Anozie, A.R. Bakare, J.A. Sonibare, and T.O. Oyebisi, *Energy* 32, 1283 (2007). 625
4. J. Parikh, K. Balakrishnan, V. Laxmi, and H. Biswas, *Energy* 26, 949 (2001). 626
5. A. Haines, K.R. Smith, D. Anderson, P.R. Epstein, A.J. McMichael, I. Roberts, P. Wilkinson, J. Woodcock, and J. Woods, *Lancet* 370, 1264 (2007). 627
6. Telecom Regulatory Authority of India, Highlights of Telecom Subscription Data as on 30 June 2011, Press release. <http://www.telecomindiaonline.com/highlights-of-telecom-subscription-data-as-on-30th-june-2011.pdf>. 628
7. The World Bank, Brazil background study for a national rural electrification strategy: aiming for universal access energy (Washington, DC: The International Bank for Reconstruction and Development/The World Bank, 2005). <http://www.esmap.org/esmap/node/338>. 629
8. M.R. Nouni, S.C. Mullick, and T.C. Kandpal, *Renew Sustain Energy Rev* 12, 1187 (2008). 630
9. D. Champier, J.P. Bédécarrats, M. Rivaletto, and F. Strub, *Energy* 35, 935 (2010). 631
10. D. Champier, J.P. Bédécarrats, T. Kousksou, M. Rivaletto, F. Strub, and P. Pignolet, *Energy* 36, 1518 (2011). 632
11. J.P. Ferrieux and F. Forest, *Alimentations à découpage, convertisseurs à résonance*, edt Dunod, ISBN: 2100041371 (2006). 633
12. C. Cabal (Ph.D. thesis, Université Paul Sabatier, Toulouse IL, 2008). 634
13. XXXX. 635

625  
626  
627  
628  
629  
630  
631  
632  
633  
634  
635  
636  
637  
638  
639  
640  
641  
642  
643  
644  
645  
646  
647  
648  
649  
650  
651  
652  
653  
654

